Synthesis and Biological Evaluation of *N*-Pyrazolyl-*N*′-alkyl/benzyl/phenylureas: a New Class of Potent Inhibitors of Interleukin 8-Induced Neutrophil Chemotaxis

Olga Bruno,*[,†] Chiara Brullo,[†] Francesco Bondavalli,[†] Silvia Schenone,[†] Angelo Ranise,[†] Nicoletta Arduino,[‡] Maria B. Bertolotto,[‡] Fabrizio Montecucco,[‡] Luciano Ottonello,[‡] Franco Dallegri,[‡] Massimiliano Tognolini,[§] Vigilio Ballabeni,[§] Simona Bertoni,[§] and Elisabetta Barocelli[§]

Dipartimento di Scienze Farmaceutiche, University of Genoa, v.le Benedetto XV, 3−Genoa, Italy, Dipartimento di Medicina Interna, University of Genoa, v.le Benedetto XV, 6−Genoa, Italy, and Dipartimento di Scienze Farmacologiche, Biologiche e Chimiche Applicate, Università degli Studi di Parma, V.le GP Usberti, 27/A−Parma, Italy

Received April 13, 2007

Neutrophils chemotaxis is a complex multistep process that, if upregulated, causes acute inflammation and a number of autoimmune diseases. We report here the synthesis of a new *N*-(4-substituted)pyrazolyl-*N*′-alkyl/benzyl/phenylureas that are potent inhibitors of interleukin-8 (IL8)-induced neutrophil chemotaxis. The first series of compounds, obtained by functionalization with a urea moiety of the 5-amino-1-(2-hydroxy-2-phenylethyl)-1*H*-pyrazole-4-carboxylic acid ethyl ester **3**, blocked the IL8-induced neutrophil chemotaxis, while they did not block *N*-formylmethionylleucylphenylalanine-mediated chemotaxis. The most active compounds, 3-benzyl- (**4d**), 3-(4-benzylpiperazinyl)- (**4i**), 3-phenyl- (**4k**) and 3-isopropylureido (**4a**) derivatives, showed an IC_{50} of 10, 14, 45, and 55 nM, respectively. Several different molecules were then synthesized to obtain more information for SAR study. Compounds **4a**, **4d**, and **4k** were inactive in the binding assays on CXCR1 and CXCR2 (IL8 receptors), whereas they inhibited the phosphorylation of PTKs (protein tyrosine kinases) in the 50−70 kDa region. Moreover, in the presence of the same derivatives, we observed a complete block of F-actin rise and pseudopod formation.

Introduction

Inflammation is the first response of the immune system to infection or irritation.[1] Generally, the inflammation results in connective tissue scarring. Nevertheless, if the injurious agent continues or the control of cellular recruitment breaks down, both acute and chronic autoimmune inflammatory disorders (such as asthma, rheumatoid arthritis, multiple sclerosis, and inflammatory bowel disease) will ensue.

Neutrophils are the main cells infiltrated in the course of acute inflammation. Their activation consists of various events: margination (rolling and adhesion to vessel walls), diapedesis (transmigration across the endothelial barrier), chemotaxis (migration to site of inflammation) and phagocytosis of foreign particles, and reactive free radicals production.[2,3]

Chemotaxis is a multistep process[4] induced by various chemoattractants such as fMLP,[a,5,6] PAF,[7] LTB4,[8] C5a anaphylotoxin[9] and different chemokines such as the CC chemokine MIP 1β or the CXC chemokine IL8 (also named CXCL8).[10]

Both IL8 and fMLP responses are induced by activation of specific G-protein-coupled receptors, which are expressed on target cells.[11−16]

Downstream of heterotrimeric G-proteins, a number of intracellular signaling systems are activated including (a) stimulation of PLC, followed by PKC activation and increasing in cytosolic calcium; (b) activation of the enzyme PI3K, resulting in increase of PIP3 and PIP2; and (c) activation of small GTP-binding proteins of the Rho family and of the MAPK cascade, as well as activation of PTKs and protein phosphatases.[17]

This complex system results in the rapid development of ruffles on the cell body and in the rise of polymerized F-actin in the ruffles. Then, the cells develop a polarized shape with formation of a contracted tail in the rear and F-actin-rich ruffles at the front.[18−20] Newly polymerized actin filaments are enriched in the leading edge of a migrating cell,[21,22] and the increase in filamentous actin causes pseudopod formation.[23−25] The block of actin polymerization abolishes chemotaxis.[26−29]

The mechanism of F-actin polymerization is not yet completely understood;[30] it depends on PI3K activation, particularly on phosphorylation of PI3Kγ[31,32] and PI3Kδ[33] isoforms, and PIP3 production; moreover, the activation of Akt/PKB is a major downstream regulator of PI3K-dependent chemotaxis.[4,34,35]

Recently, two distinct pathways of actin polymerization were reported. The PI3K-dependent signaling depends on PKC-ζ and Akt; in contrast, the PI3K-independent signaling depends on ROCK kinase, Src family tyrosine kinases, and NADPH, and it is modulated by cAMP. These distinct pathways are used by the different chemotactic receptors.[36,37]

Recently, many academic medicinal chemists and pharmaceutical research divisions have been greatly involved in the search for new molecules able to interfere with the neutrophil upregulation.

SB 225002 [*N*-(2-hydroxy-4-nitrophenyl)-*N*′-(2-bromophenyl)urea] (Figure 1) was first reported as a potent and selective

* Corresponding author. Tel: +39 010 353 8367. Fax: +39 010 353 8358. E-mail: obruno@unige.it.

† Dipartimento di Scienze Farmaceutiche, University of Genoa.

‡ Dipartimento di Medicina Interna, University of Genoa.

§ Dipartimento di Scienze Farmacologiche, Biologiche e Chimiche Applicate, Università degli Studi di Parma.

[a] Abbreviations: IL8/CXCL8, interleukin 8; Akt/PKB, protein kinase B; BSA, bovine serum albumin; CCR1/CCR2/CCR3, CC chemokine receptors; CXCR1, CXCR2, interleukin 8 receptors; ERK1/2, extracellular signal-regulated kinase 1/2; Fgr, fetal growth restriction; fMLP, *N*-formylmethionylleucylphenylalanine; HBSS, Hank's balanced salt solution; HcK, hematopoietic cell kinase; JNK1/2, c-Jun N-terminal kinase 1/2; LTB4, leukotriene B4; MAPK, mitogen-activated protein kinase; MIP1b, macrophage inflammatory protein 1b; PAF, platelet activating factor; PBS, Dulbecco's phosphate-buffered saline; PI3K, phosphoinositide 3-kinase; PIP2, phosphatidylinositol 3,4-biphosphate; PIP3, phosphatidylinositol 3,4,5-triphosphate; PLC, phospholipase C; PKC, protein kinase C; PTKs, protein kinases; pyk2, proline-rich tyrosine kinase 2; Rho, Ras homology gene; ROCK, RhoA/Rho-kinase; SRC, sarcoma; Zap-70, ζ-associated protein 70.

10.1021/jm0704402 CCC: $37.00
Published on Web 07/04/2007

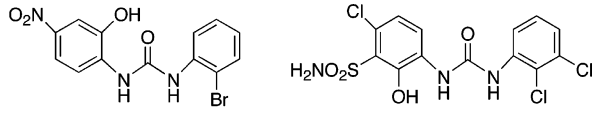

Figure 1. Structures of some CXC receptors inhibitors.

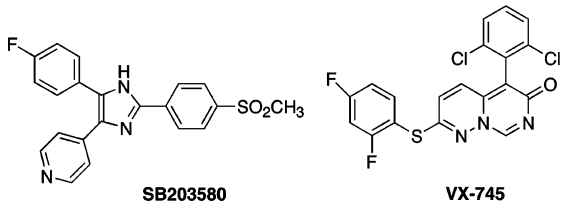

Figure 2. Structures of some p38Ks inhibitors.

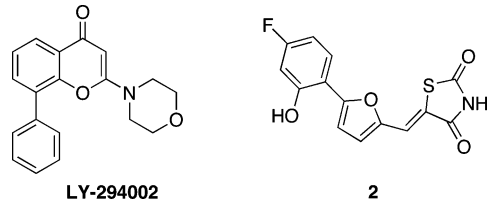

Figure 3. Structures of some PI3Ks inhibitors.

nonpeptide IL8 inhibitor binding to CXCR2.[38] It was followed by many small molecules belonging to different chemical series, acting at CXC receptors,[39,40] some of which also showed interesting pharmacological activities in vivo (see as example *N*-(3-(aminosulfonyl)-4-chloro-2-hydroxyphenyl)-*N*′-(2,3-dichlorophenyl)urea **1**, Figure 1).[41,42]

The inhibition of intracellular chemokine-activated signaling is another possible strategy. In this context, several potent p38MAPK inhibitors (see as example SB203580 or VX-745 in Figure 2)[43] were efficacious in disease models, including inflammation,[44] arthritis,[45] and pulmonary injury.[46]

Now, the goal of researchers is to identify selective inhibitors for the PI3K isoforms.[47] LY294002 (see Figure 3) was the first synthetic molecule known to inhibit PI3Ks. Currently, the PI3K inhibitors can be divided into two classes: derivatives of LY294002 and unrelated structures, which are the major part (see for example the late reported compounds **2** in Figure 3).[48]

For a long time we have been carrying out the synthesis of new heterocycle derivatives as potential anti-inflammatory agents.[49−53] Now we have focused our interest on the identification of new molecules able to impact neutrophil activation and migration.[54]

In pursuing the search for new small molecules active in this field, we functionalized with a urea moiety the 5-amino-1-(2-hydroxy-2-phenylethyl)-1*H*-pyrazole-4-carboxylic acid ethyl ester **3**, already used as a crucial intermediate,[55] and we obtained derivatives **4a**−**k** (Table 1).

To evaluate the role of the substituent in position 4 of the pyrazole moiety, in compounds **5a**−**d** we replaced the 4-carboxyethyl group with other ones, maintaining as ureido substituents the aliphatic (isopropyl) or the aromatic (phenyl) group.

Finally, to investigate the influence of electron-donor or electron-drawing substituents in the phenyl- and benzylurea moiety, we synthesized new 4-carboxyethyl derivatives (compounds **6a**−**k** and **7a**−**i**).

Chemistry

5-Amino-1-(2-hydroxy-2-phenylethyl)-*1H*-pyrazole-4-carboxylic acid ethyl ester **3** was prepared by condensation of 2-hydrazino-1-phenylethanol with ethyl ethoxymethylenecyanoacetate in anhydrous toluene, as previously reported.[55] Starting from this intermediate, we synthesized most of the title compounds following method A or method B (see Scheme 1). The former is a one-pot reaction that needs a preliminary treatment with phosgene in anhydrous THF at reflux; later, the suitable amines were added to the mixture to give compounds **4a**−**j** and **7a**−**i**. In the second way (method B), compound **3** was refluxed in anhydrous toluene with a little excess of the appropriate phenyl isocyanate to yield compounds **4k** and **6a**−**k**. IR and ^{1}H NMR spectral data confirmed the urea structure and excluded the involvement of the 2-hydroxy-2-phenylethyl group. On the other hand, we already evidenced this occurrence in analogous reactions of compound **3** with different electrophiles.[56,57]

Starting from compound **4a** we obtained in good yield compound **5a** by a simple basic hydrolysis of the 4-carboxyethyl

Table 1. Chemical Structures of Title Compounds and Chemotaxis Inhibition Values[a]

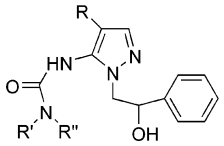

compd	R	NR′R″	inhibn of IL8-induced neutrophil migration, IC_{50} (μM)
4a	$COOC_2H_5$	$NHCH(CH_3)_2$	0.055 ± 0.021
4b	$COOC_2H_5$	1-cyclopropylamino	5.52 ± 2.313
4c	$COOC_2H_5$	$NH(CH_2)_2OCH_2CH_3$	1.00 ± 0.14
4d	$COOC_2H_5$	$NHCH_2C_6H_5$	0.010 ± 0.005
4e	$COOC_2H_5$	$NHCH_2CH_2C_6H_5$	0.61 ± 0.25
4f	$COOC_2H_5$	1-pyrrolidinyl	4.95 ± 1.669
4g	$COOC_2H_5$	1-piperidinyl	3.090 ± 1.341
4h	$COOC_2H_5$	1-(4-methylpiperazinyl)	0.865 ± 0.453
4i	$COOC_2H_5$	1-(4-benzylpiperazinyl)	0.014 ± 0.007
4j	$COOC_2H_5$	4-morpholinyl	0.95 ± 0.341
4k	$COOC_2H_5$	NHC_6H_5	0.045 ± 0.007
5a	COOH	$NHCH(CH_3)_2$	0.251 ± 0.035
5b	H	$NHCH(CH_3)_2$	0.825 ± 0.021
5c	CN	$NHCH(CH_3)_2$	0.035 ± 0.021
5d	CN	NHC_6H_5	0.225 ± 0.007
6a	$COOC_2H_5$	$NHC_6H_4F(o)$	0.033 ± 0.006
6b	$COOC_2H_5$	$NHC_6H_4F(m)$	0.036 ± 0.002
6c	$COOC_2H_5$	$NHC_6H_4F(p)$	0.033 ± 0.001
6d	$COOC_2H_5$	$NHC_6H_4Cl(m)$	1.560 ± 0.19
6e	$COOC_2H_5$	$NHC_6H_4Cl(p)$	0.345 ± 0.11
6f	$COOC_2H_5$	$NHC_6H_4Br(m)$	0.424 ± 0.013
6g	$COOC_2H_5$	$NHC_6H_4Br(p)$	0.092 ± 0.008
6h	$COOC_2H_5$	$NHC_6H_4CH_3(m)$	0.398 ± 0.009
6i	$COOC_2H_5$	$NHC_6H_4CH_3(p)$	0.445 ± 0.027
6j	$COOC_2H_5$	$NHC_6H_4OCH_3(o)$	1.20 ± 0.05
6k	$COOC_2H_5$	$NHC_6H_4OCH_3(m)$	1.40 ± 0.20
7a	$COOC_2H_5$	$NHCH_2C_6H_4F(o)$	1.487 ± 0.344
7b	$COOC_2H_5$	$NHCH_2C_6H_4F(m)$	0.318 ± 0.053
7c	$COOC_2H_5$	$NHCH_2C_6H_4F(p)$	0.212 ± 0.033
7d	$COOC_2H_5$	$NHCH_2C_6H_4Cl(o)$	1.244 ± 0.255
7e	$COOC_2H_5$	$NHCH_2C_6H_4Cl(m)$	0.570 ± 0.080
7f	$COOC_2H_5$	$NHCH_2C_6H_4Cl(p)$	0.935 ± 0.167
7g	$COOC_2H_5$	$NHCH_2C_6H_4Br(o)$	1.777 ± 0.086
7h	$COOC_2H_5$	$NHCH_2C_6H_4Br(m)$	0.198 ± 0.024
7i	$COOC_2H_5$	$NHCH_2C_6H_4Br(p)$	3.886 ± 0.039

[a] Neutrophils chemotaxis was evaluated in a Boyden chamber assays, as described in the Experimental Section, after stimulation with 10^{-8} M IL8 or 10^{-9} M fMLP, in the absence and presence of tested compounds. The net migration was determined by subtracting spontaneous migration, i.e., the distance travelled by neutrophils in the absence of the stimulus, from the distance travelled by neutrophils toward the stimulus. The concentration of each compound giving 50% inhibition (IC_{50}) of net migration was obtained from nonlinear regression analysis, and the results reported are the mean of at least three experiments. No inhibitory activity was observed in fMLP-induced chemotaxis.

Scheme 1. Synthesis of Compounds **4a**−**k**, **6a**−**k**, and **7a**−**i**[a]

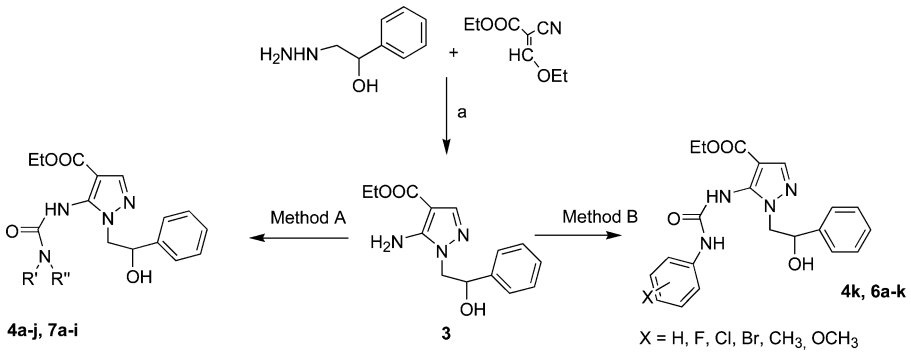

[a] Reagents: (a) anhyd toluene, reflux, 8 h. Method A, step1: $COCl_2$, anhyd AcONa, anhyd THF, reflux, 4 h; step 2: excess of primary or secondary amines, anhyd THF, rt, 12 h. Method B: suitable phenyl isocyanate, anhyd toluene, reflux, 6 h.

Scheme 2. Synthesis of Compounds **5a,b**[a]

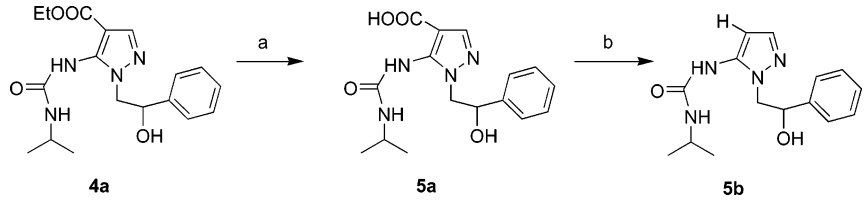

[a] Reagents: (a) Step 1: NaOH, EtOH, reflux, 2 h. Step 2: H_3O^+. (b) Heating at 165 °C.

Scheme 3. Synthesis of Compounds **8**, **5c**, and **5d**[a]

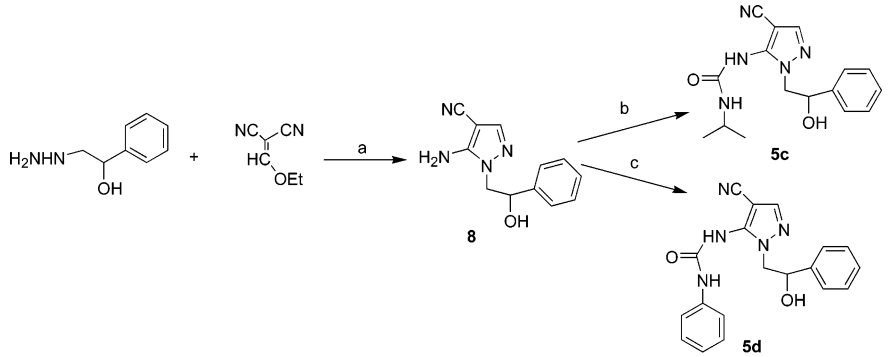

[a] Reagents: (a) ethanol, reflux, 8 h. (b) Step1: $COCl_2$, anhyd AcONa, anhyd THF, reflux, 4 h. Step 2: excess of isopropylamine, anhyd THF, rt, 12 h. (c) Phenyl isocyanate, anhyd toluene, reflux, 6 h.

group (Scheme 2). The following decarboxylation at high temperature gives compound **5b**. For compounds **5c** and **5d**, we prepared the new intermediate, 5-amino-1-(2-hydroxy-2-phenylethyl)-1*H*-pyrazole-4-carbonitrile **8**, by condensation of 2-hydrazino-1-phenylethanol with ethoxymethylenemalononitrile in absolute ethanol (Scheme 3). Then, method A or method B was applied to obtain compound **5c** or **5d**, respectively.

Biological Studies

All synthesized compounds were tested to evaluate the inhibition of IL8- and fMLP-induced neutrophil migration. To establish the role of the ureido group in the chemotaxis inhibition, we tested, in the same assays, the intermediate 5-amino pyrazole **3** also.

The interesting results obtained in the functional IL8-induced chemotactic test, and the nearly complete inability to interfere in the fMLP-induced chemotaxis, prompted us to examine the possible interaction of our compounds with the IL8 receptors (CXCR1 and CXCR2). The negative response of the binding assays suggested a likely interference in the intracellular signal transduction pathways. As reported in the introduction section, this is a very complex sequence of reactions in which a series of serine-threonine or tyrosine protein kinases are involved.

It has been reported that the phosphotyrosine content of several proteins in the 60−70, 100, and 120 kDa regions rapidly increases in IL8-stimulated neutrophils.[58] Thus, we tested the most active compounds, **4a**, **4d**, and **4k**, in an immunoblotting test of IL8-induced tyrosine phosphorylation. The study showed a certain ability to reduce the phosphorylation in the 60−70 and 50 kDa regions (see Figures 4 and 5).

Consequently, we submitted the same compounds to a binding assay on a series of tyrosine (unspecific SRC, Fgr, Hck, Zap-70) kinases having a molecular weight in the cited regions; in addition, we tested them on some serine-threonine (p38α, p38β2, p38δ, p38γ, ERK1, ERK2, JNK1, JNK2, pKB/Akt1) kinases, selected as among the most involved in the neutrophils action, to confirm a kinase inhibition and a possible selectivity.

In addition, we also determined the content of F-actin in IL8-stimulated neutrophils, in the absence and presence of compounds **4a**, **4d**, and **4k**. An additional test of Akt phosphorylation was performed to verify the involvement of the same compounds in the PI3K-dependent actin polymerization.

Finally, some of the most active compounds (**4a**, **4d**, **4h**, **4i**, **4k**, **6a**, **6b**, and **6c**) were preliminarly tested in vivo in a mouse model of zymosan-induced peritonitis.

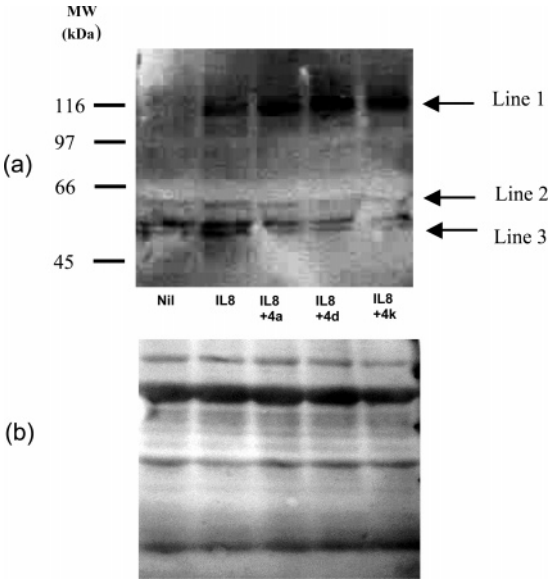

Figure 4. (a) Effect of compounds **4a**, **4d**, and **4k** on the tyrosine phosphorylation in human neutrophils stimulated with IL8 for 0.5 min. The three compounds reduce tyrosine phosphorylation (lines 2 and 3) but are ineffective on the phosphorylation of 100−120 kDa proteins (line 1). (b) To verify equal protein amount in the different samples, nitrocellulose membrane was stained with Ponceau S.

Results

No compounds, at the used concentrations, showed cytotoxic activity toward neutrophils, the percentage of viable cells never being lower than 90%.

All tested compounds, except the 5-aminopyrazole **3**, blocked the IL8-induced neutrophil chemotaxis, while they were inactive toward fMLP. In the first series, the most active were the 3-benzyl-, 3-(4-benzylpiperazinyl)-, 3-phenyl-, and 3-isopropylureido derivatives (**4d**, **4i**, **4k**, and **4a**) with an IC_{50} of 10, 14, 45, and 55 nM, respectively (Table 1). On the other hand, compounds **4e** and **4j** also showed a very interesting activity, having an IC_{50} of 0.61 and 0.95 μM, respectively, while compounds **4b**, **4c**, **4f**, and **4g** were the least active, with IC_{50} ranging from 1.00 to 5.52 μM.

These preliminary data allowed us to underline the crucial role of the urea group and their substituents. First, compound **3**, devoid of ureido function, was completely unable to block the neutrophil migration. Moreover, the presence of an aromatic moiety (phenyl, benzyl, or 4-benzylpiperazinyl) gave very potent compounds, but the 3-isopropylureido derivative **4a** also showed a very strong activity.

Hydrolysis or complete removal of the 4-carboxyethyl group was detrimental for the chemotaxis inhibition. In fact, in the 3-isopropylureido derivatives, IC_{50} increases from 55 nM (compound **4a**) to 250 and 825 nM (compounds **5a** and **5b**, respectively). The substitution of 4-carboxyethyl with a 4-cyano group did not give clear information: in the 3-isopropylureido derivative (**5c**), the activity slightly increases (IC_{50} being 35 nM versus 55 nM for the analogue **4a**); in contrast, in the 3-phenylureido derivative (**5d**) the potency decreases (IC_{50} being 225 nM versus 45 nM for the analogue **4k**). Thus, we suppose that a substituent in position 4 of the pyrazole is needed, but further investigations are required to clarify which is the better one.

Electron-donor substituents in the phenylureido moiety strongly decreased the activity: in fact, compounds **6h**−**k** showed IC_{50} values 10−30-fold higher than the analogue **4k**.

Of the electron-withdrawing substituents (Br, Cl, F) only fluorine, whether in the ortho, meta, or para position, slightly increased the activity compared to the unsubstituted **4k** (see compounds **6a**−**c**). These data suggested that a detrimental steric hindrance nullifies the favorable electronic effect.

Finally, in the last series of 3-benzylureido derivatives, all the substitutions were detrimental for the activity, compounds **7a**−**i** having an IC_{50} ranging from 0.2 to 3.8 μM, about 20−40-fold higher than the unsubstituted **4d** (one of the most active compounds previously synthesized).

Some compounds (**4a**, **4d**, **4k**) selected among the most active in the migration test were submitted to a binding assay on CXCR1, CXCR2, CCR1, CCR2, and CCR3, but they were completely inactive (data not shown).

Stimulation of neutrophils with 10^{-7} M IL8 very rapidly increased the phosphotyrosine content of proteins in the 60−70 and 50 kDa regions; moreover, the immunoblotting test also evidenced a strong stimulation in the 116 KDa region (see line 1 in Figure 4), corresponding to proline-rich tyrosine kinase pyk2, already reported as one of the possible targets of neutrophil chemotaxis inhibitors.[59] Interestingly, the pretreatment

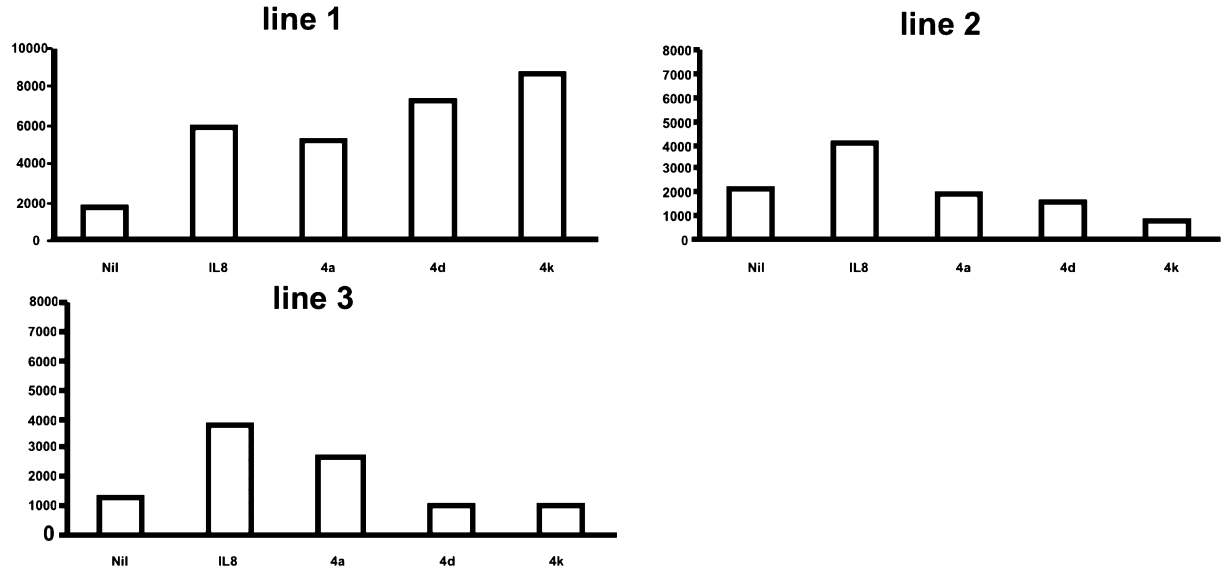

Figure 5. Densitometric analysis of Western blot for tyrosine phosphorylation in human neutrophils stimulated with IL8 for 0.5 min. Densitometric analysis was carried out using the slab shown in Figure 4. Each panel shows analysis of the lines 1, 2, and 3 of the slab, respectively.

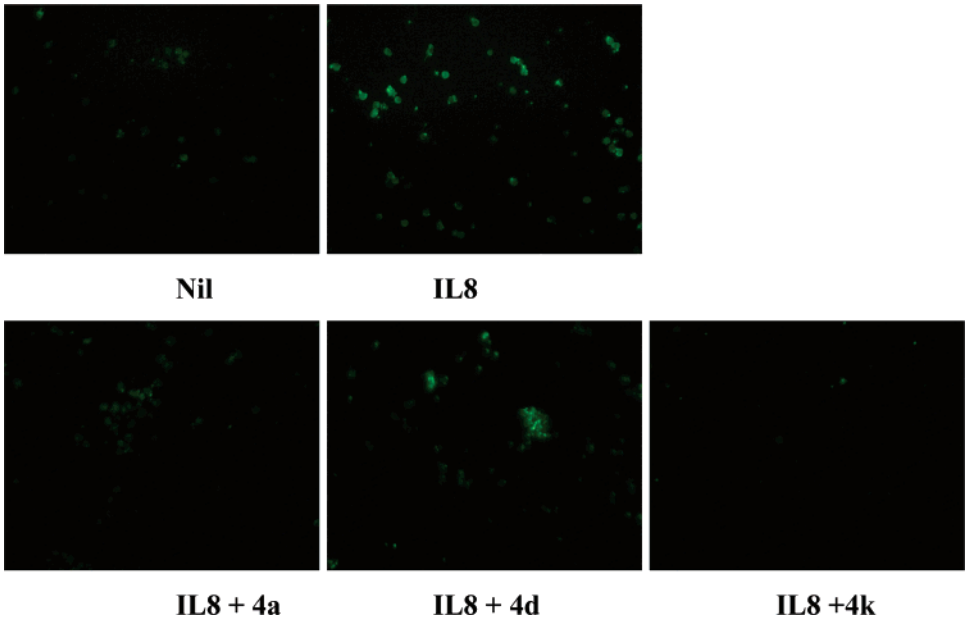

Figure 6. Determination of F-actin content in neutrophils stimulated with IL8 in the absence and presence of compounds **4a**, **4d**, and **4k**. F-actin was stained with alexa-Fluor 488-conjugated phalloidin. The content of F-actin was determined by fluorescence microscopy as described in the Experimental Section. The figures are representative of three independent experiments.

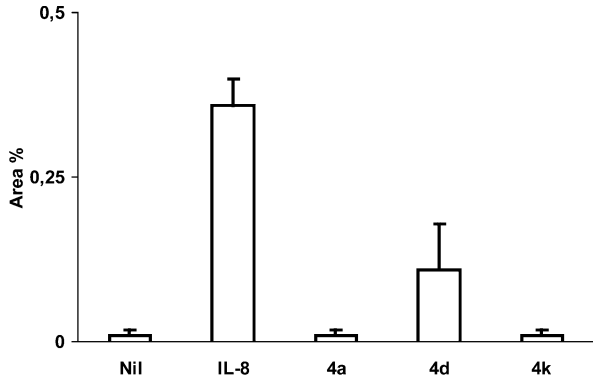

Figure 7. Determination of F-actin content in neutrophils IL8 stimulated in the absence and presence of compounds **4a**, **4d**, and **4k.** Analysis of the slides reported in Figure 6. The mean fluorescence density was determined from a linear measurement of individual cell fluorescence. Results are shown as the mean ± SD of the fluorescence densities expressed as area percentage of each field for each individual slide.

with compounds **4a**, **4d**, and **4k** reduced the tyrosine phosphorylation in the 60−70 and 50 kDa regions (see image in Figure 4 and densitometric analysis in Figure 5). In particular, line 2 evidenced 53%, 63%, and 81% reduction for compound **4a**, **4d**, and **4k**, respectively; line 3 showed 20%, 70%, and 71% reduction for compound **4a**, **4d**, and **4k**, respectively. In contrast, in line 1 we observed a slight increase of phosphorylation; however, we cannot clearly relate this behavior to the chemotaxis inhibition. Moreover, all the binding tests on the tyrosine kinases having MW ranging from 50 to 70 kDa (unspecific SRC, Fgr, Hck, Zap-70) as well as those on the serine-threonine kinases (p38α, p38β2, p38δ, p38γ, ERK1, ERK2, JNK1, JNK2, Akt1) were negative.

Compounds **4a**, **4d**, and **4k** also reduced the content of polymerized actin in IL8-stimulated neutrophils (as shown in Figures 6 and 7) 97%, 69%, and 97%, respectively.

However, the Western blot on Akt phosphorylation showed a complete inactivity of tested compounds (data not shown). On the other hand, compounds **4a**, **4d**, and **4k** were inactive in the binding test on Akt enzyme, confirming the absence of activity toward this serine-threonine-kinases-dependent pathway.

Table 2. Effect of Compound **6b** on Cell and Granulocyte Recruitment Induced by Zymosan in Mouse[a]

compounds	no. peritoneal cells (% inhibn)	no. peritoneal granulocytes (% inhibn)	% mono-cytes	% lympho-cytes	% granulo-cytes
vehicle			9	25	66
6b (100 mg/kg os)	29*	33*	10	28	62
dexamethasone (1 mg/kg os)	36*	62**	14	44	42

[a] Animals received the compound under study (100 mg/kg os) or dexamethasone (1 mg/kg os) 1 h before intraperitoneal injection of zymosan (1 mg/mouse). Peritoneal fluid was collected and examined microscopically 4 h later. *$p < 0.05$, **$p < 0.01$ by Student's *t*-test compared to vehicle-treated mice.

Concerning the in vivo assay, most of the tested compounds (**4a**, **4d**, **4h**, **4i**, **4k**, **6c**, **6a**) did not modify the inflammatory response induced by zymosan intraperitoneal injection. Protein content of peritoneal cavity lavage was similar in vehicle- or compound-treated mice. In contrast, treatment with compound **6b** caused a significant decrease of cells and granulocytes present in the peritoneal cavity compared to vehicle-treated mice (Table 2).

Conclusions

In conclusion, we reported the synthesis of a large series of *N*-pyrazolyl-*N*′-substituted ureas that strongly inhibited IL8-induced neutrophils recruitment. The most active compounds were the 3-benzyl-, 3-(4-benzylpiperazinyl)-, 3-phenyl-, 3-(fluoro)phenyl, and the 3-isopropylureido derivatives, having a carboxyethyl group in position 4 of the pyrazole moiety. These compounds were inactive toward the CXC receptors.

The involvement of the synthesized compounds in the complex intracellular mechanisms of neutrophil recruitment was confirmed by the determination of F-actin content: in fact, a remarkable decrease was noted in the presence of tested compounds. The negative test on Akt phosphorylation, con-

firmed by the negative result of the binding assay on Akt, indicates that our compounds inhibit the actin polymerization by a PI3K-independent mechanism.

The inhibition of tyrosine phosphorylation in the 50−70 kDa region, evidenced by the immunoblotting test, suggests that our compounds act toward one or more of the numerous kinases involved in these complex cascade-activation processes. However, the screening of a large number of kinases enzyme assays showed negative results; thus, the exact molecular target is not yet known.

In the preliminary in vivo test, only the 3-fluorophenyl derivative **6b** showed a good inhibition of neutrophils chemotaxis. It is worth nothing that the unsubstituted analogue **4k**, which showed a comparable activity in vitro, was inactive in vivo. Consequently, we assume that a fluorine in the phenyl ring is important to achieve activity in vivo.

These results prompted us to pursue the synthetic work, to obtain new derivatives that are more potent in vivo, and to plan in-depth biological analyses to clarify the mechanism of action.

Experimental Section

Chemical Materials and Methods. All chemicals were obtained from Sigma-Aldrich s.r.l. (Milan, Italy).

Melting points are not corrected and were measured with a Büchi 540 instrument. IR spectra were recorded with a Perkin-Elmer 398 spectrophotometer. ^{1}H NMR spectra were recorded on a Varian Gemini 200 (200 MHz) instrument; chemical shifts are reported as δ (ppm) relative to tetramethylsilane (TMS) as internal standard; signals were characterized as s (singlet), d (doublet), t (triplet), q (quartet), sept (septet), m (multiplet), or br s (broad signal); *J* are reported in hertz.

All compounds were tested for purity by TLC (Kieselgel 60F254 DC-Alufolien, E. Merck, Darmstadt, Germany).

Elemental analyses, indicated by the symbols of the elements, were within ±0.4% of the theoretical values and were determined with an EA 1110 elemental analyzer (Fison-Instruments, Milan, Italy).

General Procedure for 1-(2-Hydroxy-2-phenylethyl)-5-(3-alkyl/cycloalkylureido)-*1H*-pyrazole-4-carboxylic Acid Ethyl Esters 4a−j and 1-(2-Hydroxy-2-phenylethyl)-5-(3-benzylureido)-*1H*-pyrazole-4-carboxylic Acid Ethyl Esters 7a−i (Method A). To a mixture of ethyl 5-amino-1-(2-hydroxy-2-phenylethyl)-1*H*-pyrazole-4-carboxylate **3** (2.7 g, 10 mmol) and anhydrous CH_3COONa (2.0 g, 24 mmol) in anhydrous THF (30 mL), at 0 °C, was added dropwise phosgene (20% in toluene, 8 mL) and then the reaction mixture was heated at reflux for 4 h. After removal in vacuo of the excess phosgene, the suitable amine (25 mmol), solved in anhydrous THF, was added dropwise at 0 °C; the mixture was stirred at room temperature overnight. After removal of the volatiles in vacuo, the crude was suspended in water (20 mL), extracted twice with CH_2Cl_2 (20 mL), and dried ($MgSO_4$). The solvent was evaporated under reduced pressure to give yellow oils, which were crystallized with diethyl ether. All products were purified by recrystallization from absolute ethanol.

Analytical data for compounds **4a−j** and **7a−i** are available as Supporting Information.

General Procedure for 1-(2-Hydroxy-2-phenylethyl)-5-(3-phenylureido)-1*H*-pyrazole-4-carboxylic Acid Ethyl Esters 4k and 6a−k (Method B). A mixture of 5-amino-1-(2-hydroxy-2-phenylethyl)-1*H*-pyrazole-4-carboxylic acid ethyl ester **3** (2.7 g, 10 mmol) and the suitable phenyl isocyanate (11 mmol) in anhydrous toluene (30 mL) was refluxed for 6 h. After cooling, the white solids obtained were filtered and recrystallized from absolute ethanol.

Analytical data for compounds **4k** and **6a−k** are available as Supporting Information.

Synthesis and Analytical Data of 1-(2-Hydroxy-2-phenylethyl)-5-(3-isopropylureido)-1*H*-pyrazole-4-carboxylic Acid 5a. To a solution of 1-(2-hydroxy-2-phenylethyl)-5-(3-isopropylureido)-1*H*-pyrazole-4-carboxylic acid ethyl ester **4a** (1.8 g, 5 mmol) in 95% ethanol (9 mL) was added 2 M NaOH (9 mL) and the mixture was heated at reflux for 2 h. After removal of ethanol in vacuo, the crude was dissolved in water (20 mL) and then the basic solution was washed with $CHCl_3$ (20 mL) and made acid with 6 N HCl to afford a white solid, which was filtered and recrystallized by absolute ethanol. Yield: 91%. Mp: 163−164 °C. IR (KBr) cm^{-1}: 3449, 3400, 3324, 3232 (OH, NH), 1697 (CO), 1655 (CON). ^{1}H NMR (DMSO-d_6): δ 0.97 (d, J = 4.0, 3H, CH_3CH), 0.99 (d, J = 4.0, 3H, CH_3CH), 3.88−4.39 (m, 2H, CH_2N), 4.83−5.01 (m, 1H, *CH*NH), 5.64−5.75 (m, 1H, disappears with D_2O), 5.84−6.00 (m, 1H, *CH*OH), 6.05−6.20 (m, 2H, disappears with D_2O), 7.02−7.50 (m, 6H, 5Ar + H-3), 11.75 (s, 1H, COOH, disappears with D_2O). Anal. ($C_{16}H_{20}N_4O_4$) C, H, N.

Synthesis and Analytical Data of 2-[5-(3-Isopropylureido)-pyrazol-1-yl]-1-phenylethan-1-ol 5b. Compound **5a** (1.30 g, 4 mmol) was heated at 165 °C until complete development of CO_2; the residue was cooled to room temperature and purified by Florisil (100−200 mesh) chromatography using CH_2Cl_2 as eluent. The white solid obtained was recrystallized from absolute ethanol. Yield: 17%. Mp: 136−137 °C. IR (KBr) cm^{-1}: 3392, 3320, 3215 (OH, NH), 1711 (CON). ^{1}H NMR (DMSO-d_6): δ 1.05−1.18 (m, 6H, 2CH_3), 3.28−3.46 (m, 2H, disappears with D_2O), 3.46−3.84 (m, 1H, *CH*NH), 4.27−4.60 (m, 2H, CH_2N), 4.90−4.95 (m, 1H, disappears with D_2O), 5.48 (d, J = 4.0, 1H, H-4), 5.90−6.00 (m, 1H, *CH*OH), 6.21 (d, J = 4.0, 1H, H-3), 7.23−7.40 (m, 5H, Ar). Anal. ($C_{15}H_{20}N_4O_2$) C, H, N.

Synthesis and Analytical Data of 5-Amino-1-(2-hydroxy-2-phenylethyl)-1*H*-pyrazole-4-carbonitrile 8. To a solution of 2-hydrazino-1-phenylethanol (6.08 g, 40 mmol) in absolute ethanol (50 mL) was added ethoxymethylenemalononitrile (4.88 g, 40 mmol) and the reaction mixture was refluxed for 6 h. The solvent was concentrated to 50% of the initial volume and cooled. The yellow solid obtained was filtered and recrystallized from absolute ethanol. Yield: 63%. Mp: 180−181 °C. IR (KBr) cm^{-1}: 3438, 3339, 3199 (OH, NH_2), 2223 (CN). ^{1}H NMR ($CDCl_3$): δ 3.15 (br s, 1H, OH, disappears with D_2O), 3.98−4.27 (m, 2H, CH_2N), 4.80 (br s, 2H, NH_2, disappears with D_2O), 5.08−5.18 (m, 1H, *CH*OH), 7.26−7.45 (m, 5H, Ar), 7.46 (s, 1H, H-3). Anal. ($C_{12}H_{12}N_4O$) C, H, N.

Synthesis and Analytical Data of 1-(2-Hydroxy-2-phenylethyl)-5-(3-isopropylureido)-1*H*-pyrazole-4-carbonitrile 5c. To a mixture of **8** (2.3 g, 10 mmol) and anhydrous CH_3COONa (2.0 g, 24 mmol) in anhydrous THF (30 mL), cooled at 0 °C, was added phosgene (20% in toluene, 8 mL) dropwise, and the reaction mixture was refluxed for 4 h. The excess phosgene was removed under reduced pressure and isopropylamine (1.48 g, 25 mmol), solved in anhydrous THF (5 mL), was added dropwise, at 0 °C. The mixture reaction was stirred at room temperature overnight. After removal of the volatiles in vacuo, the crude was suspended in water (20 mL) and extracted twice with CH_2Cl_2 (20 mL), and the organic phase was dried ($MgSO_4$). The solvent was evaporated under reduced pressure to afford a yellow oil, which was purified by Florisil (100−200 mesh) chromatography using diethyl ether as eluent. Yield: 57%. Mp: 170 °C. IR (KBr) cm^{-1}: 3306, 3229, 3194 (OH, NH), 2229 (CN), 1683 (CO). ^{1}H NMR ($CDCl_3$): δ 1.08 and 1.12 (dd, J = 5.6, 6H, CH_3), 2.60−3.00 (m, 2H, 2NH, disappears with D_2O), 3.75−3.94 (m, 1H, *CH*NH), 4.04−4.14 (m, 2H, CH_2N), 4.96−5.08 (m, 1H, *CH*OH), 6.06 (d, J = 6.0, 1H, OH, disappears with D_2O), 7.18−7.37 (m, 5H, Ar), 7.62 (s, 1H, H-3). Anal. ($C_{16}H_{19}N_5O_2$) C, H, N.

Synthesis and Analytical Data of 1-(2-Hydroxy-2-phenylethyl)-5-(3-phenylureido)-1*H*-pyrazole-4-carbonitrile 5d. A solution of **8** (2.3 g, 10 mmol) and phenyl isocyanate (1.2 g, 11 mmol) in anhydrous toluene (30 mL) was refluxed for 6 h. After cooling, the white solid obtained was filtered and recrystallized from absolute ethanol. Yield: 78%. Mp: 214−215 °C. IR (KBr) cm^{-1}: 3385, 3283, 3202 (NH, OH), 2226 (CN), 1715 (CON). ^{1}H NMR (DMSO-

d_6): 3.36 (d, $J = 1.8$, 1H, OH, disappears with D_2O), 4.18−4.50 (m, 2H, CH_2N), 6.05−6.17 (m, 1H, *CH*OH), 6.65 (br s, 1H, NH, disappears with D_2O), 6.90−7.50 (m, 10H, Ar), 7.54 (s, 1H, H-3), 9.73 (br s, 1H, NH, disappears with D_2O). Anal. ($C_{19}H_{17}N_5O_2$) C, H, N.

Biological Materials and Methods. Hank's balanced salt solution without phenol red (HBSS, ICN Biomed, Milan, Italy) mixed with Dulbecco's phosphate-buffered saline (PBS, ICN Biomed) (HBSS:PBS = 3:1) containing 1 mg/mL bovine serum albumin (BSA, Sigma, Milan, Italy) was used as incubation medium. fMLP, IL8, ethidium bromide, and fluorescein diacetate were from Sigma Chemical, St. Louis, MO.

Neutrophilic Polymorphonuclear Leukocyte Preparation. Heparinized venous blood (10 U/mL heparin) was obtained from healthy volunteers (20−37 yr old) after informed consent. Neutrophilic polymorphonuclear leukocytes (neutrophils) were prepared by dextran sedimentation, followed by centrifugation (400*g*, 30 min) on a Ficoll-Hypaque density gradient, as previously described.[60] Contaminating erythrocytes were removed by hypotonic lysis. Neutrophils resuspended in incubation medium were >97% pure, as determined by morphologic analysis of Giemsa-stained cytopreparation.

Assessment of Neutrophil Viability. Neutrophils (2×10^6/mL) were incubated for 2 h in tissue culture tubes (17 × 100 mm, Falcon, Becton Dickinson) in incubation medium at 37 °C in a CO_2 atmosphere (0.5 mL final volume), with appropriate doses of compounds **3**, **4a**−**k**, **5a**−**d**, **6a**−**k**, and **7a**−**i**. Cell viability, measured as integrity of membrane, was assessed by an ethidium bromide−fluorescein diacetate test according to Dankberg[61] as previously described by Ottonello.[62] Briefly, cells (4×10^4/100 mL) harvested from culture tubes were mixed with 50 mL of staining solution (2 mg/mL fluorescein diacetate, 4 μg/mL ethidium bromide) in HBSS and incubated for 10 min at room temperature. Thereafter, a drop of cell suspension was placed on a slide, sealed with a coverslip, and analyzed under UV light in a dark field illumination. Neutrophils with intact membrane (i.e., viable cells) appeared as green fluorescent cells, whereas neutrophils with damage and ethidium bromide-permeable membrane (i.e., necrotic cells) displayed a fluorescent red nucleus.

Boyden Chamber Migration Assay. Neutrophil locomotion was studied by means of the leading front method, as previously described by Corcione.[63] Neutrophils were preincubated in the absence or presence of appropriate doses of compounds **3**, **4a**−**k**, **5a**−**d**, **6a**−**k**, and **7a**−**i**, for 15 min at room temperature. Tests were conducted in duplicate, using blind well chambers (Neuro-Probe, Gathersburg, MD) with a 3 μm pore size cellulose ester filter (Millipore, Milan, Italy) separating the upper from the lower compartment of the chambers. Then cells (4×10^5), in the absence or presence of various amounts of tested compounds, were placed in the upper compartment of the chambers. Chemoattractants, 10^{-9} M IL8 or 10^{-8} M fMLP, were placed in the lower compartment of the chambers. Experiments were also carried out without chemoattractants in the lower compartment (spontaneous migration). After incubation at 37 °C for 45 min, the filters were removed, fixed in ethanol, stained with Harris hematoxylin, dehydrated, cleared with xylene, and mounted in Eukitt (Kindler, GmbH). Then, the distance (mm) travelled by the leading front of cells was measured × 400 magnification. Five randomly chosen fields were read for each filter. The net migration was determined by subtracting spontaneous migration, i.e., the distance travelled by neutrophils in the absence of the stimulus, from the distance travelled by neutrophils toward the stimulus. The concentration of each compound giving 50% inhibition (IC_{50}) of net migration was obtained from nonlinear regression analysis with SPSS for Windows version 6.0, Wacker Drive, Chicago, IL.

IL8-Induced Tyrosine Phosphorylation in Human Neutrophils. Western blot analysis was carried out as previously described.[64] Neutrophils were incubated at 2.5 × 107 cells/mL with 10^{-3} M diisopropylfluorophosphate for 30 min at room temperature. The cells were then incubated with or without compounds **4a** (0.06 μM), **4d** (0.01 μM), and **4k** (0.05 μM) for 30 min and subsequently stimulated with 10^{-7} M IL8 for 0.5 min. The reactions were stopped by transferring 100 mL of each sample in an equivalent volume of sample buffer (Tris-HCl, pH 6.8, 2 mmol/L Na_3VO_4, 10^{-3} M PMSF, 10 μg/mL aprotinin, 10 μg/mL leupeptin, 8% sodium dodecyl sulfate (SDS), 10% mercaptoethanol, 17.5% glycerol, and 0.1% bromophenol blue) prewarmed to 95 °C. The samples were denatured by boiling for 10 min and then were loaded onto 7.5%−20% SDS polyacrylamide gel. After the electrophoresis, the proteins were transferred on nitrocellulose membrane at 4 °C for 45 min at 240 mA. The blots were blocked with 5% non-fat dry milk and washed in Tris-buffered saline/Tween 20 (TBS-T, containing 10 mM Tris-base pH 7.4, 154 mM NaCl, and 0.05% Tween 20). The membranes were stained with μg/mL anti-phosphotyrosine mAb clone 4G10 (Upstate) (overnight incubation at 4 °C). After washing with TBS-T, the membranes were incubated with anti-mouse horseradish peroxidase-linked anti-IgG Ab. The membranes were washed again under the same conditions, and antibody complexes were visualized by the enhanced chemiluminescence (ECL) detection system (Amersham, Little Chalfont, U.K.) according to the manufacturer's instructions.

IL8-Induced Akt Phosphorylation in Human Neutrophils. Western blot analysis was carried out as previously described.[64] After purification, neutrophils (1×10^7cells/mL) were pretreated with compounds **4a** (0.06 μM), **4d** (0.01 μM), and **4k** (0.05 μM), for 30 min, and then they were incubated in air at 37 °C in the absence or presence of 10 nM IL8 for 5 min. The reaction was stopped on ice, and the cells were centrifugated at 4 °C. After removing the supernatants, the pellets were lysed in 400 μL of NP40 buffer (20 mM Tris-HCl, pH 7.5, 150 mM NaCl, 10 mM NaF, 1% NP40, 10 μg/mL glycerol, 10 μg/mL aprotinin, 10 μg/mL leupeptin, 1 mM PMSF, 0.5 mM Na_3VO_4) and incubated for 30 min at 4 °C. The samples were spun at 13 000*g* for 10 min at 4 °C. Protein content was determined with BCA protein assay (Pierce) using bovine serum albumin as standard. The cytoplasmic extracts were boiled in loading buffer (62.5 mM Tris-HCl pH 6.8, 0.75% SDS, 3.75% 2-mercaptoethanol, 8.75% glycerol, and 0.025% bromophenol blue) and then resolved by SDS−polyacrilamide electrophoresis (5% stacking gel and 12% running gel). After the electrophoresis, the proteins (40 g each sample) were transferred on nitrocellulose membrane at 4 °C for 45 min at 240 mA. The blots were blocked with 5% non-fat dry milk and washed in Tris-buffered saline/Tween 20 (TBS-T, containing 10 mM Tris-base pH 7.4, 154 mM NaCl, and 0.05% Tween 20). The membranes were stained with μg/mL anti-human phosphorylated Akt mAb (Santa Cruz Biotechnology) (overnight incubation at 4 °C). After washing with TBS-T, the membranes were incubated with anti-rabbit horseradish peroxidase-linked anti-IgG Ab. The membranes were washed again under the same conditions, and antibody complexes were visualized by the enhanced chemiluminescence (ECL) detection system (Amersham, Little Chalfont, U.K.) according to the manufacturer's instructions.

Densitometric and Statistical Analysis. Images of blots were analyzed by scanning densitometry quantified with the image analyzer system (Syngene). Data were expressed as mean ± SEM. One-way ANOVA with Bonferroni's post-test was performed using GraphPad InStat version 3.05 for Windows XP, GraphPad Software (San Diego, CA). Differences between treatment groups were judged to be statistically significant at $p < 0.05$.

Determination of the Total Cellular F-Actin. After the isolation from blood from young healthy volunteers, neutrophils were tested in the presence or absence of compounds **4a**, **4d**, and **4k**. After the incubation, neutrophils were washed three times and then stimulated for 30 min with control medium or 100 nM IL8. After this treatment, neutrophil slides were prepared by cytospin centrifuge, and F-actin was stained with alexa-Fluor 488-conjugated phalloidin. The content of F-actin was determined by fluorescence microscopy (Nikon Optiphot-2, Nikon, Melville, NY). Image capturing was performed with a Hamamatsu color-chilled 3 CCD camera. All images were captured using identical camera settings (time of exposure, brightness, contrast and sharpness) and an appropriated white balance set according to the fluorescence filter and acquired and analyzed by Image-Pro Plus 4.0 (from Media Cybernetics).

The mean fluorescence density was determined from a linear measurement of individual cell fluorescence. All cells of at least five randomly chosen fields of each slide, performed in duplicate, were analyzed from at least three individual experiments. Results are shown as the mean ± SD of the mean fluorescence densities expressed as the area percentage of each field for each individual slide. Figures show representative images taken by Adobe Photoshop Software (Adobe System, San Jose, CA).

Induction of Peritonitis, Cell Count, Cell Composition, and Determination of Protein Concentration in the Peritoneal Exudate. The experiments were performed using male Swiss mice (25−30 g) fasted 16 h before the experiment, but with free access to water. Mice were randomly assigned to groups of eight animals orally treated with vehicle or the compounds under examination (100 mg/kg os) 1 h before the induction of peritonitis. Dexamethasone (1 mg/kg os) was used as reference drug. Peritonitis was induced following a modification of Thurmond's method.[65] Briefly, 5 mg/mL zymosan or phosphate-buffered saline (PBS) was injected into the peritoneal space of mice (final volume 0.2 mL). After 4 h, the animals were euthanized, and the peritoneal cavities were washed with 3 mL of PBS containing 3 mM EDTA, and the volume was collected with automatic pipettes. Total leukocyte counts were performed in a Neubauer chamber by means of optical microscopy after diluting a sample of the peritoneal fluid with Türk solution (1:100). Differential cell counts were performed using a light microscope. Neutrophils were easily differentiated by their chromatic characteristics and the shape of the nucleus relative to the cytoplasm.

Protein content was spectrophotometrically determined following the bicinchonate method with a commercial kit (Pierce, BCA protein assay kit). Experiments were carried out in accordance with Italian law (DL 116/92) and approved by the Ministry of Health.

Acknowledgment. The authors wish to thank Dr. R. Raggio, Mr. O. Gagliardo, and F. Tuberoni for spectral recording. We also thank Prof. M. Bradley for the English revision of the text. Financial support from University of Genoa is gratefully acknowledged.

Supporting Information Available: Yields, melting point, IR and ^{1}H NMR spectral data of compounds **4a**−**k**, **6a**−**k**, **7a**−**i** and elemental analyses table of all synthesized compounds. This material is available free of charge via the Internet at http://pubs.acs.org.

References

(1) Nauseef, W. M.; Clark, R. A. In *Basic Principles in the Diagnosis and Management of Infectious Diseases. 1*; Mandel, G. L., Bennett, J. E., Dolin, R., Eds.; Churchill Livingstone: New York, 2000; pp 89−112.
(2) Kobayashi, S. D.; Voyich, J. M.; De Leo, F. R. Regulation of the neutrophil mediated inflammatory response to infection. *Microbes Infect*. **2003**, *5*, 1337−1344.
(3) Delves, P. J.; Roitt, I. M. The immune system. Second of two parts. *Adv. Immunol*. **2000**, *343*, 108−117.
(4) Katanaev, V. L. Signal transduction in neutrophil chemotaxis. *Biochemistry* **2001**, *66*, 351−368.
(5) Panaro, M. A.; Mitolo, V. Cellular responses to FMLP challenging: A mini-review. *Immunopharmacol. Immunotoxicol*. **1999**, *21*, 397−419.
(6) Selvatici, R.; Falzarano, S.; Mollica, A.; Spisani, S. Signal transduction pathways triggered by selective formylpeptide analogues in human neutrophils. *Eur. J. Pharmacol.* **2006**, *534*, 1−11.
(7) Hanahan, D. J. Platelet activating factor: A biologically active phosphoglyceride. *Annu. Rev. Biochem*. **1986**, *55*, 483−509.
(8) Crooks, S. W.; Stockley, R. A. Leukotriene B4. *Int. J. Biochem. Cell Biol*. **1998**, *30*, 173−178.
(9) Gerard, C.; Gerard, N. P. C5a anaphylatoxin and its seven transmembrane-segment receptor. *Annu. Rev. Immunol.* **1994**, *12*, 775−808.
(10) Baggiolini, M. Chemokines and leukocyte traffic. *Nature* **1998**, *392*, 565−568.
(11) Hartt, J.; Barish, G.; Murphy, P. M.; Gao, J. L. *N*-Formylpeptides induce two distinct concentration optima for mouse neutrophil chemotaxis by differential interaction with two N-formylpeptide receptor (FPR) subtypes: Molecular characterization of FPR2, a second mouse neutrophil FPR. *J. Exp. Med*. **1999**, *190*, 741−747.
(12) Le, Y.; Oppenheim, J. J.; Wang, J. M. Pleitropic roles of formyl peptide receptors. *Cytokine Growth Factor Rev.* **2001**, *12*, 91−105.
(13) Holmes, W. E.; Lee, J.; Kuang, W. J.; Rice, G. C.; Wood, W. I. Structure and functional expression of a human interleukin-8 receptor. *Science* **1991**, *253*, 1278−1280.
(14) Murphy, P. M.; Tiffany, H. L. Cloning of complementary DNA encoding a functional human interleukin-8 receptor. *Science* **1991**, *253*, 1280−1283.
(15) Zlotnik, A.; Yoshie, O. Chemokines: A new classification system and their role in immunity. *Immunity* **2000**, *12*, 121−127.
(16) Chuntharapai, A.; Kim, J. K. Regulation of the expression of IL8 receptor A/B by IL8: Possible functions of each receptor. *J. Immunol.* **1995**, *155*, 2587−2594.
(17) Niggli, V. Signaling to migration in neutrophils: Importance of localized pathways. *IJBCB* **2003**, *35*, 1619−1638.
(18) Cicchetti, G.; Allen, P. G.; Glogauer, M. Chemotactic signaling pathways in neutrophils: From receptor to actin assembly. *Crit. Rev. Oral Biol. Med.* **2002**, *13*, 220−228.
(19) Stephens, L.; Ellson, C.; Hawkins, P. Roles of PI3Ks in leukocyte chemotaxis and phagocytosis. *Curr. Opin. Cell Biol.* **2002**, *14*, 203−213.
(20) Weiner, O. D. Regulation of cell polarity during eukaryotic chemotaxis: The chemotactic compass. *Curr. Opin. Cell Biol.* **2002**, *14*, 196−202.
(21) Fechheimer, M.; Zigmond, S. H. Changes in cytoskeletal proteins of polymorphonuclear leukocytes induced by chemotactic peptides. *Cell Motil.* **1983**, *3*, 349−361.
(22) Valerius, N. H.; Stendahl, O.; Hartwig, J. H.; Stossel, T. P. Distribution of actin-binding protein and myosin in polymorphonuclear leukocytes during locomotion and phagocytosis. *Cell* **1981**, *24*, 195−202.
(23) Wymann, M. P.; Kernen, P.; Bengtsson, T.; Andersson, T.; Baggiolini, M.; Deranleau, D. A. Corresponding oscillations in neutrophil shape and filamentous actin content. *J. Biol. Chem*. **1990**, *265*, 619−622.
(24) Condeelis, J. Life at the leading edge: The formation of cell protrusions. *Annu. Rev. Cell Biol.* **1993**, *9*, 411−444.
(25) Elson, E. L.; Felder, S. F.; Jay, P. Y.; Kolodney, M. S.; Pasternak, C. Forces in cell locomotion. *Biochem. Soc. Symp.* **1999**, *65*, 299−314.
(26) Carter, S. B. Effects of cytochalasins on mammalian cells. *Nature* **1967**, *213*, 261−264.
(27) Becker, E. L.; Davis, A. T.; Estensen, R. D.; Quie, P. G. Cytochalasin B. IV. Inhibition and stimulation of chemotaxis of rabbit and human polymorphonuclear leukocytes. *J. Immunol.* **1972**, *108*, 396−402.
(28) Zigmond, S. H.; Hirsch, J. G. Effects of cytochalasin B on polymorphonuclear leucocyte locomotion, phagocytosis and glycolysis. *Exp. Cell Res.* **1972**, *73*, 383−393.
(29) Norgauer, J.; Kownatzki, E.; Seifert, R.; Aktories, K. Botulinum C2 toxin ADP-ribosylates actin and enhances O^{2-} production and secretion but inhibits migration of activated human neutrophils. *J. Clin. Invest.* **1988**, *82*, 1376−1382.
(30) Pollard, T. D.; Blanchoin, L.; Mullins, R. D. Molecular mechanisms controlling actin filament dynamics in nonmuscle cells. *Annu. Rev. Biophys. Biomol. Struct*. **2000**, *29*, 545−576.
(31) Li, Z.; Jiang, H.; Xie, W.; Zhang, Z.; Smrcka, A. V.; Wu, D. Roles of PLC-beta2 and -beta3 and PI3Kgamma in chemoattractant-mediated signal transduction. *Science* **2000**, *287*, 1046−1049.
(32) Hirsch, E.; Katanaev, V. L.; Garlanda, C.; Azzolino, O.; Pirola, L.; Silengo, L.; Sozzani, S.; Mantovani, A.; Altruda, F.; Wymann, M. P. Central role for G protein-coupled phosphoinositide 3-kinase gamma in inflammation. *Science* **2000**, *287*, 1049−1053.
(33) Sadhu, C.; Masinovsky, B.; Dick, K.; Sowell, C. G.; Staunton, D. E. Essential role of phosphoinositide 3-kinase δ in neutrophil directional movement. *J. Immunol.* **2003**, *170*, 2647−2654.
(34) Wang, F.; Herzmark, P.; Weiner, O. D.; Srinivasan, S.; Servant, G.; Bourne, H. R. Lipid products of PI(3)Ks maintain persistent cell polarity and directed motility in neutrophils. *Nat. Cell Biol.* **2002**, *4*, 513−518.
(35) Chodniewicz, D.; Zhelev, D. V. Novel pathways of F-actin polymerization in the human neutrophil. *Blood* **2003**, *102*, 2251−2258.
(36) Chodniewicz, D.; Zhelev, D. V. Chemoattractant receptor-stimulated F-actin polymerization in the human neutrophil is signaled by 2 distinct pathways. *Blood* **2003**, *101*, 1181−1184.
(37) Zhelev, D. V.; Alteraifi, A. M.; Chodniewicz, D. Controlled pseudopod extension of human neutrophils stimulated with different chemoattractants. *Biophys. J.* **2004**, *87*, 688−695.
(38) White, J. R.; Lee, J. M.; Young, P. R.; Hertzberg, R. P.; Jurewicz, A. J.; Chaikin, M. A.; Widdowson, K. L.; Foley, J. J.; Martin, L. D.; Griswold, D. E.; Sarau, H. M. Identification of a potent, selective non-peptide CXCR2 antagonist that inhibits interleukin-8-induced neutrophil migration. *J. Biol. Chem.* **1998**, *273*, 10095−10098.
(39) Horuk, R. Chemokine receptor antagonists. *Med. Res. Rev.* **2000**, *20*, 155−168.

(40) Johnson, Z.; Power, C. A.; Weiss, C.; Rintele, F.; Ji, H.; Rickle, T.; Camps, M.; Wells, T. N. C.; Schwarz, M. K.; Poudfoot, A. E. I.; Rommel, C. Chemokine inhibition—Why, when, where, which and how? *Biochem. Soc. Trans.* **2004**, *32*, 366−377.
(41) Podolin, P. L.; Bolognese, B. J.; Foley, J. J.; Schmidt, D. B.; Buckley, P. T.; Widdowson, K. L.; Jin, Q.; White, J. R.; Lee, J. M.; Goodman, R. B.; Hagen, T. R.; Kajikawa, O.; Marshall, L. A.; Hay, D. W. P.; Sarau, H. M. A Potent and selective nonpeptide antagonist of CXCR2 inhibits acute and chronic models of arthritis in the rabbit. *J. Immunol.* **2002**, *169*, 6435−6444.
(42) Souza, D. G.; Bertini, R.; Vieira, A. T.; Cunha, F. Q.; Poole, S.; Allegretti, M.; Colotta, F.; Teixeira, M. M. Repertaxin, a novel inhibitor of rat CXCR2 function, inhibits inflammatory responses that follow intestinal ischemia and reperfusion injury. *Br. J. Pharmacol.* **2004**, *143*, 132−142.
(43) Lee, J. C.; Kumar, S.; Griswold, D. E.; Underwood, D. C.; Votta, B. J.; Adams, J. L. Inhibition of p38 MAP kinase as therapeutic strategy. *Immunopharm.* **2000**, *47*, 185−201.
(44) Ottosen, E. R.; Sorensen, M. D.; Björkling, F.; Skak-Nielsen, T.; Fjording, S. M.; Aaes, H.; Binderup, L. Synthesis and Structure−activity relationship of aminobenzophenones. A novel class of p38 MAP kinase inhibitors with high antiinflammatory activity. *J. Med. Chem.* **2003**, *46*, 5651−5662.
(45) Redman, A. M.; Johonson, J. S.; Dally, R.; Swartz, S.; Wild, H.; Paulsen, H.; Caringal, Y.; Gunn, D.; Renick, J.; Osterhout, M.; Kingery-Wood, J.; Smith, R. A.; Lee, W.; Dumas, J.; Wilhelm, S. M.; Housley, T. J.; Bhargava, A.; Ranges, G. E.; Shrikhande, A.; Young, D.; Bombara, M.; Scott, W. J. p38 Kinase inhibitors for the treatment of arthritis and osteoporosis: Thienyl, furyl and pyrrolyl ureas. *Bioorg. Med. Chem. Lett.* **2001**, *11*, 9−12.
(46) Nick, J. A.; Young, S. K.; Arndt, P. G.; Lieber, J. G.; Suratt, B. T.; Poch, K. R.; Avdi, N. J.; Malcolm, K. C.; Taube, C.; Henson, P. M.; Worthen, G. S. Selective suppression of neutrophil accumulation in ongoing pulmonary inflammation by systemic inhibition of p38 mitogen-activated protein kinase1. *J. Immunol.* **2002**, *169*, 5260−5269.
(47) Ward, S.; Sotsios, Y.; Dowden, J.; Bruce, I.; Finan, P. Therapeutic potential of phosphoinositide 3-kinase inhibitors. *Chem. Biol.* **2003**, *10*, 207−213.
(48) Pomel, V.; Klicic, J.; Covini, D.; Church, D. D.; Shaw, J. P.; Roulin, K.; Burgat-Charvillon, F.; Valognes, D.; Camps, M.; Chabert, C.; Gillieron, C.; Françon, B.; Perrin, D.; Leroy, D.; Gretener, D.; Nichols, A.; Vitte, P. A.; Carboni, S.; Rommel, C.; Schwarz, M. K.; Rückle, T. Furan-2-ylmethylene thiazolidinediones as novel, potent, and selective inhibitors of phosphoinositide 3-kinase γ. *J. Med. Chem.* **2006**, *49*, 3857−3871.
(49) Bruno, O.; Ranise, A.; Bondavalli, F.; Schenone, P.; D'Amico, M.; Lampa, E.; Falzarano, C.; Rossi, F. 3,5-Diphenyl-*1H*-pyrazole derivatives X. N-substituted 1-(2-aminopropyl)- and 1-(3-amino-2-hydroxypropyl)-3,5-diphenyl-*1H*-pyrazoles with antiinflammatory and other activities, *Farmaco* **1992**, *47*, 1235−1248.
(50) Bruno, O.; Ranise, A.; Bondavalli, F.; Schenone, P.; D'Amico, M.; Filippelli, A.; Filippelli, W.; Rossi, F. 3,5-diphenyl-*1H*-pyrazole derivatives. XI. *N*-Aryl-5(3)-phenyl-4-(3,5-diphenyl-1-pyrazolyl)-3(5)-pyrazoleamines, 5-substituted 4,5-dihydro-3-phenyl-4-(3,5-diphenyl-1-pyrazolyl)-*1H*-pyrazoles and 2,6-disubstituted 1,6-dihydro-4-phenyl-5-(3,5-diphenyl-1-pyrazolyl)pyrimidines with antipyretic, antiinflammatory and other activities. *Farmaco* **1993**, *48*, 949−966.
(51) Bruno, O.; Schenone, S.; Ranise, A.; Bondavalli, F.; Filippelli, W.; Falcone, G.; Motola, G.; Mazzeo, F. Antiinflammatory agents: New series of N-substituted amino acids with complex pyrimidine structures endowed with antiphlogistic activity. *Farmaco* **1999**, *54*, 95−100.
(52) Schenone, S.; Bruno, O.; Ranise, A.; Bondavalli, F.; Falcone, G.; Filippelli, W.; Rivaldi, B. *N*-Substituted 3-(arylamino)-4,5-dihydro-*2H*-benz[*g*]indazol-2-yl acetamides with anti-inflammatory and analgesic activities. *Farmaco* **2000**, *55*, 383−388.
(53) Ranise, A.; Schenone, S.; Bruno, O.; Bondavalli, F.; Filippelli, W.; Falcone, G.; Rivaldi, B. *N*-Acyl-*N*-phenyl ureas of piperidine and substituted piperidines endowed with anti-inflammatory and antiproliferative activities. *Farmaco* **2001**, *56*, 647−657.
(54) Bruno, O.; Brullo, C.; Arduino, N.; Schenone, S.; Ranise, A.; Bondavalli, F.; Ottonello, L.; Dapino, P.; Dallegri, F. Synthesis and biological evaluation of neutrophilic inflammation inhibitors. *Farmaco* **2004**, *59*, 223−235.
(55) Schenone, S.; Bruno, O.; Fossa, P.; Ranise, A.; Menozzi, G.; Mosti, L.; Bondavalli, F.; Martini, C.; Trincavelli, L. Synthesis and biological data of 4-amino-1-(2-chloro-2-phenylethyl)-*1H*-pyrazolo[3,4-*b*]pyridine-5-carboxylic acid ethyl esters, a new series of A_1-adenosine receptor (A_1AR) ligands. *Bioorg. Med. Chem. Lett.* **2001**, *11*, 2529−2531.
(56) Schenone, S.; Bruno, O.; Bondavalli, F.; Ranise, A.; Mosti, L.; Menozzi, G.; Fossa, P.; Manetti, F.; Morbidelli, L.; Trincavelli, L.; Martini, C.; Lucacchini, A. 1-(2-chloro-2-phenylethyl)-6-methylthio-*1H*-pyrazolo[3,4-*d*]pyrimidines 4-amino substituted and their pharmacological evaluation. *Eur. J. Med. Chem.* **2004**, *39*, 153−160.
(57) Schenone, S.; Bruno, O.; Bondavalli, F.; Ranise, A.; Mosti, L.; Menozzi, G.; Fossa, P.; Donnini, S.; Santoro, A.; Ziche, M.; Manetti, F.; Botta, M. Antiproliferative activity of new 1-aryl-4-amino-*1H*-pyrazolo[3,4-*d*]pyrimidine derivatives toward the human epidermoid carcinoma A431 cell line. *Eur. J. Med. Chem.* **2004**, *39*, 939−946.
(58) L'Heureux, G. P.; Bourgoin, S.; Jean, N.; McColl, S. R.; Naccache, P. H. Diverging signal transduction pathways activated by interleukin-8 and related chemokines in human neutrophils: Interleukin-8, but not NAP-2 or GRO alpha, stimulates phospholipase D activity. *Blood* **1995**, *85*, 522−531.
(59) Di Cioccio, V.; Strippoli, R.; Bizzarri, C.; Troiani, G.; Cervellera, M. N.; Gloaguen, I.; Colagrande, A.; Catozza, E. M.; Pagliei, S.; Santoni, A.; Colotta, F.; Mainero, F.; Bertini, R. Key role of proline rich tyrosine kinase 2 in interleukine 8 (CXCL8/IL8)-mediated human neutrophil chemotaxis. *Immunol.* **2004**, *111*, 407−415.
(60) Ottonello, L.; Morone, P.; Dapino, P.; Dallegri, F. Monoclonal Lym-1 antibody-dependent lysis of B-lymphoblastoid tumor targets by human complement and cytokinine-exposed mononuclear and neutrophilic polymorphonuclear leukocytes. *Blood* **1996**, *87*, 5171−5178.
(61) Dankberg, F.; Perdiansky, M. A test of granulocyte membrane integrity and phagocytic function. *Cryobiology* **1976**, *13*, 430−432.
(62) Ottonello, L.; Gonella, R.; Dapino, P.; Sacchetti, C.; Dallegri, F. Prostaglandin E2 inhibits apoptosis in human neutrophilic polymorphonuclear leukocytes: Role of intracellular cyclic AMP levels. *Exp. Haematol.* **1998**, *26*, 895−902.
(63) Corcione, A.; Ottonello, L.; Tortolina, G.; Tasso, P.; Ghiotto, F.; Airoldi, I.; Taborelli, G.; Malavasi, F.; Dallegri, F.; Pistoia, V. Recombinant tumor necrosis factor enhances the locomotion of memory and naive B lymphocytes from human tonsils through the selective engagement of the type II receptor. *Blood* **1997**, *90*, 4493−4501.
(64) Ottonello, L.; Montecucco, F.; Bertolotto, M.; Arduino, N.; Mancini, M.; Corcione, A.; Pistoia, V.; Dallegri, F. CCL3 (MIP-1alpha) induces in vitro migration of GM-CSF-primed human neutrophils via CCR5-dependent activation of ERK 1/2. *Cell. Signal.* **2005**, *17*, 355−363.
(65) Thurmond, R. L.; Desai, P. J.; Dunford, P. J.; Fung-Leung, W. P.; Hofstra, C. L.; Jiang, W.; Nguyen, S.; Riley, J. P.; Sun, S.; Williams, K. N.; Edwards, J. P.; Karlsson, L. A potent and selective histamine H4 receptor antagonist with anti-inflammatory properties. *J. Pharmacol. Exp. Ther.* **2004**, *309*, 404−413.

JM0704402